ELSEVIER

Journal of Nuclear Materials 294 (2001) 223–231

journal of nuclear materials

www.elsevier.nl/locate/jnucmat

Stability of SiC/SiC fibre composites exposed to Li_4SiO_4 and Li_2TiO_3 in fusion relevant conditions

A. La Barbera [a], B. Riccardi [b,*], A. Donato [b], C.A. Nannetti [a], L.F. Moreschi [c]

[a] *ENEA INN-NUMA, CR Casaccia, S. Maria di Galeria, 00060 Rome, Italy*

[b] *Associazione EURATOM ENEA sulla Fusione, C.R. Frascati, Via E. Fermi 27, CP 65, 00044 Frascati, Rome, Italy*

[c] *Associazione EURATOM ENEA, CP 1, 40032 Camugnano, Italy*

Received 19 June 2000; accepted 3 February 2001

Abstract

The physico-chemical stability of a commercial 3D SiC_f/SiC composite provided with an outer CVD SiC protective layer was studied after exposure to flowing helium with 0.1% H_2 at 800°C in contact with lithium silicate and lithium titanate. Exposure tests were carried out for 216, 1000 and 10 000 h in an especially designed loop. The mechanical characteristics of the SiC_f/SiC composite in contact with Li_4SiO_4 were almost unaffected by the exposure, while those in contact with Li_2TiO_3 were slightly worsened. SiC coating transformation was clearly detected on samples exposed to both lithium silicate and titanate.

1. Introduction

Ceramic matrix composites (CMC) are under extensive development in order to be used as high temperature structural materials. Among them, SiC fibre–matrix ceramic composites (SiC_f/SiC composites) are interesting for fusion reactors because of their good mechanical properties at high temperatures, low chemical sputtering, high oxygen gettering and low activation at short and medium terms. Therefore, their use was proposed for some conceptual fusion reactor studies [1–3] as a blanket structural material using both liquid and solid breeders. To verify the physico-chemical and mechanical stability as well as the presence, if any, of corrosion phenomena of commercial SiC_f/SiC composites, exposure tests were carried out in the presence of lithium orthosilicate (Li_4SiO_4) and lithium titanate (Li_2TiO_3) breeder pebbles under fusion relevant conditions up to a significant exposure time. Li_4SiO_4 was chosen because it is the reference breeder material for the European helium cooled pebble bed blanket concept (HCPB) of DEMO reactor and Li_2TiO_3 because it is considered to represent the most promising alternative.

Compatibility studies of SiC_f/SiC with lithium orthosilicate under fusion relevant conditions had already been reported [4] though only for a limited exposure time; furthermore, little is known about the compatibility with lithium titanate. The present paper describes the exposure experiments carried out for 216, 1000 and 10 000 h, and reports the results of the subsequent physico-chemical and mechanical characterisation of SiC_f/SiC.

2. Experimental

2.1. Materials

2.1.1. SiC_f/SiC composite

SEP Division of SNECMA (Bordeaux, France) produced the used SiC_f/SiC composite material commercially named CERASEP© N-31. The material was obtained by the SEP chemical vapour infiltration process of 3D Nicalon CG™ fibre preforms (Guipex© texture). Nicalon fibre is a Si–O–C compound containing about 12% of oxygen. To increase the composite toughness, a 0.2 μm pyrolitic carbon interlayer at fibre–matrix interface was provided. The experimental

* Corresponding author. Tel.: +39-06 9400 5159; fax: +39-06 9400 5799.

E-mail address: riccardi@frascati.enea.it (B. Riccardi).

0022-3115/01/$ - see front matter
PII: S0022-3115(01)00487-1

Table 1
Main properties of SEP SiC_f/SiC composites

Property	Temperature (°C)	CERASEP® N2-1 (2D)	CERASEP® N3-1 (3D)
Density	20	2.5 g cm^{-3}	>2.4 g cm^{-3}
Porosity	20	10%	(10 ± 2)%
Fibre content	–	40%	40%
Tensile strength (in plane)	20	285 MPa	(300 ± 20) MPa
Tensile strain (in plane)	20	0.75	(0.8 ± 0.25)%
Young's modulus (in plane)	20	200 GPa	(200 ± 20) GPa
Trans-laminar shear strength	20	200 MPa	(200 ± 20) MPa
Inter-laminar shear strength	20	–	44 MPa
Thermal conductivity (in plane)	1000	15 W m^{-1} K^{-1}	15 W m^{-1} K^{-1}
Thermal conductivity (through the thickness)	20	9 W m^{-1} K^{-1}	(13 ± 2) W m^{-1} K^{-1}
	800	5.8 W m^{-1} K^{-1}	7.6 W m^{-1} K^{-1}
	1000	5.7 W m^{-1} K^{-1}	7.5 W m^{-1} K^{-1}
Thermal expansion coefficient (in plane)	20	4.0×10^{-6} K^{-1}	4.0×10^{-6} K^{-1}
Thermal expansion coefficient (through the thickness)	20	2.5×10^{-6} K^{-1}	–

samples were cut from large pieces into $50 \times 10 \times 3$ mm^3 bars and then subjected to a final uniform SiC coating (about 100 μm thick) by chemical vapour deposition in order to protect the bare fibres ends and fibre-coating–matrix interfaces. The general characteristics of the SiC_f/SiC material reported in Table 1 were taken from [5] and from information supplied afterwards.

Large variations in geometrical and physical properties of the as-received samples were observed. Since these large variations could mask the change of properties when considering the average values, non-destructive characterisations were performed on each individual sample before and after exposure. They included geometrical dimensions, mass variation, longitudinal and torsional dynamic moduli of elasticity (by the longitudinal and torsional fundamental resonant frequency method). Finally, the total defects population was estimated by calculating the damping constant following the Zener bandwidth method [6]. The values with their standard deviation and the variation ranges determined on the total amount of the as-received specimens are reported in Table 2. It can be seen that, in some cases, the variation ranges are broader than 2 sigma.

SEM observations on an as-received specimen are shown in Figs. 1(a) and (b). At a lower magnification (200×), it is clearly possible to distinguish between the outer fibre bundles and the SiC coated on the composite surface. At higher magnification, the microstructure of the SiC coating evidences several well-developed crystals with sharp straight edges.

2.1.2. Characteristics of Li_4SiO_4

The Li_4SiO_4 solid breeder pebbles used in the experiments were developed by Forschungzentrum Karlsruhe (FZK, Germany) [7] and industrially produced by Glaswerke Schott (Germany) by using the melt spray technique. The pebbles had an average diameter of 0.55 mm and contained 5% of SiO_2 and about 2% of TeO_2. The main physico-chemical characteristics and the chemical impurities concentrations have been reported elsewhere [7,8]. Moreover, the phases present have been identified as Li_4SiO_4, Li_2SiO_3 and Li_2TeO_3 [9].

Table 2
Main physico-chemical characteristics of CERASEP N31 specimens

	Value	Min–max
Width (mm)	9.87 ± 0.03	9.81–9.95
Thickness (mm)	3.03 ± 0.07	2.93–3.20
Length (mm)	49.79 ± 0.04	49.72–49.90
Weight (mg)	3700 ± 100	3500–4000
Density (g cm^{-3})	2.48 ± 0.03	2.42–2.53
E_{long} (GPa)	238 ± 7	222–251
G_{tors} (GPa)	91 ± 5	80–100
Damping constant ($Q^{-1} \times 10^5$)	16 ± 2	13–24

2.1.3. Characteristics of Li_2TiO_3

The general characteristics of Li_2TiO_3 pebbles to be used in a reactor blanket were not yet defined at the beginning of the tests; therefore, only baseline, mechanical and thermal properties were drawn [10]. The Li_2TiO_3 solid breeder pebbles, available at the beginning of the tests, were produced in laboratory by ENEA starting from a commercial powder of $Li_2TiO_3 +$ 0.8% TiO_2 manufactured by STREM (purity 97.5%). The pebbles were obtained by plasticising the powder with a hydroalcoholic solution of Methocel A4, by

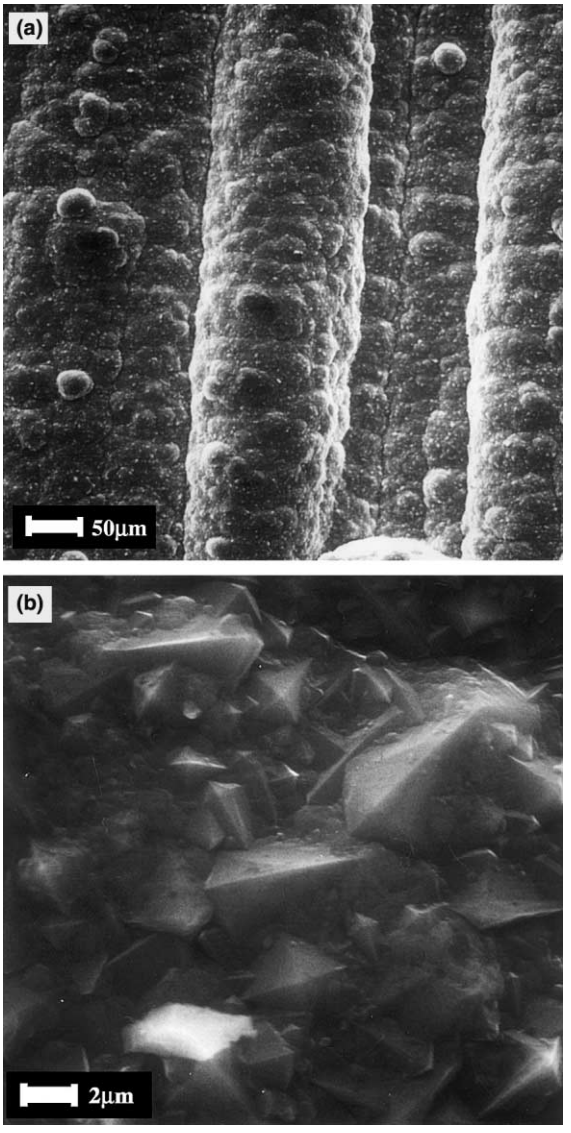

Fig. 1. SiC_f/SiC composite as-received: (a) 200×; (b) 5000×.

forming granules through a 2 mm screen and spheroidising them by simple tumbling in a planetary mill. Finally, the granules were sintered at 1300°C for 2 h. Some physico-chemical characteristics are shown in Table 3.

2.2. Experimental loop

The SiC_f/SiC specimens were exposed to flowing helium (0.1 l min^{-1}) added with 0.1% hydrogen at 800°C for 216, 1000 and 10 000 h in contact with Li_2TiO_3 and Li_4SiO_4 pebbles. These experimental conditions were chosen in order to simulate as closely as possible a blanket operating under the conditions reported in the ARIES-1 project [1], deviced with the use of SiC_f/SiC composites as structural material.

Table 3
Physical and chemical characteristics of lithium metatitanate (Li_2TiO_3)

ø pebbles (mm)	0.5–2.0
Density (g cm^{-3})	1.22 (60% TD)[a]
Main phase	Li_2TiO_3
Total impurity (%)	2.58
Al (%)	1.70
Zr (%)	0.70
Na (%)	0.05
Mg (%)	0.07
K (%)	0.06
Others	ppm level

[a] TD, theoretical density; impurity level by nuclear activation analysis.

For the exposure experiments, six completely welded test chambers made of Inconel 600 were used. A schematic view of one of them is shown in Fig. 2. The test chambers were divided into three zones, separated by gas-permeable porous Inconel walls (Poral). The helium gas flowing from the bottom of the chamber through the lower porous separator, was diffused through the breeder bed and the SiC_f/SiC specimens placed at its core, and then went out through the upper porous separator and the upper zone of the chamber, where blank specimens were also placed in order to evaluate the stability of the material that was not in direct contact with the breeder materials.

The test chambers (three of them filled with Li_2TiO_3 and three with Li_4SiO_4 pebbles beds) were placed in an

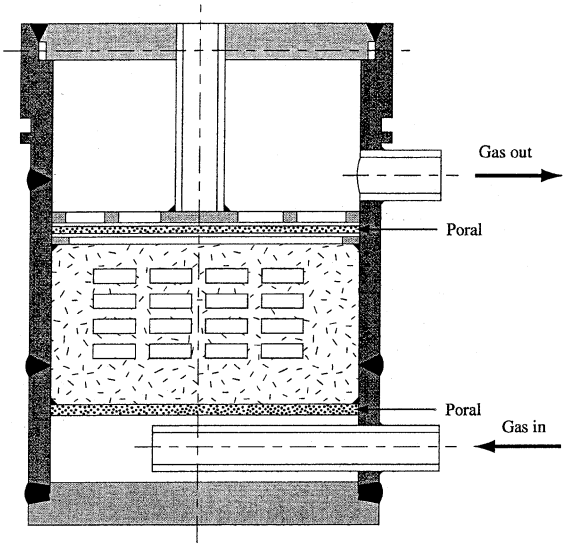

Fig. 2. A schematic view of the exposure test chambers.

oven, connected to the gas line (pressure = 1 bar) and then flushed with the above-mentioned gas which contained 20–30 vppm of water vapour before heating up to the test temperature.

3. Results and discussion

The as-received as well as the exposed specimens were characterised regarding the mechanical and physico-chemical point of view in order to evaluate the material stability and the presence, if any, of corrosion phenomena as well as their importance. The following characteristics were considered:

(a) Mechanical properties, using the three-point bending test at room temperature, 400°C and 800°C, on 10 specimens for each condition for statistic evaluation.
(b) Static and dynamic elastic properties.
(c) Scanning electron microscopy (SEM) and X-ray diffraction (XRD).
(d) Surface analysis.

The as-received samples were characterised at RT, 400°C and 800°C and their data were considered as reference ones. Only one blank and two immersed specimens were selected to follow points b, c and d.

3.1. Exposure in lithium silicate pebble beds

The immersed SiC_f/SiC samples with masses of about 3–4 g showed increasing weight in time, as reported in Table 4. It was also observed that the density did not significantly change until up to 1000 h of exposure, while a maximum weight increase of 2.5% was detected after 10 000 h. SEM examination of samples after 216 h evidenced a finer structure and a smoother aspect of the surface with respect to the original one. After 1000 h, the samples surface showed drastic morphological changes: large spherical protuberances with a diameter of 50 μm and more were detected; the original SiC coating appeared completely hidden (Fig. 3) by a cracked scale which tended to grow and coarsen after 10 000 h. The cross-section of an immersed specimen exposed for 10 000 h is shown in Fig. 4. Practically no changes were detected in the core of the specimen. The outer SiC coating was still present although with a slightly reduced thickness (ranging from 80 to 100 μm). The heavily cracked and scarcely adherent surface scale was observed all over the sample and presented an almost constant thickness of about 30 μm. The surface scale, already present and identified as Li_2SiO_3 by XRD analysis after 216 h, tended to grow markedly with exposure time as evaluated by semiquantitative XRD analysis.

Blank samples showed a very slight increasing weight in time, as reported in Table 4. However, SEM examinations showed a change in the morphological aspect of the SiC coating even after 216 h of exposure. In fact, the sharp straight edges of the SiC crystals observed in as-received material were no longer present in these specimens, indicating a starting transformation process (Fig. 5). After 1000 h, the surface appeared drastically changed due to a partial filling of the space between the bundles, that tends to mask the cloth texture morphology of the original surface. Moreover, the scale formed appeared cracked (Fig. 6). After 10 000 h, the surface appeared vitrified and much more coarsened. XRD analyses evidenced only the silica phase and SiC after 1000 h while Li_2SiO_3 and $Li_2Si_2O_5$ in addition to silica were formed on specimens exposed for 10 000 h.

3.1.1. Mechanical properties

Concerning the elastic properties and the damping constant, no significant changes were observed until up to 1000 h of exposure, in spite of the drastic morphological changes above described. Only a small worsening of the dynamic Young's modulus (3.9% and 6.6%) and of the torsional modulus (11.9% and 7.3%) was detected after 10 000 h. Moreover, the damping constant variations (84% and 92.2%) were not sufficiently high to be considered significant.

Table 4
Weight and density variation of blank and immersed specimens in Li_4SiO_4

Specimen	Exposure time (h)	Weight variation (mg)	Weight variation (%)	Density variation (%)
A	216	+6.6	+0.17	n.s.[a]
B	216	+8.3	+0.23	n.s.
C	1000	+19.0	+0.52	n.s.
D	1000	+22.3	+0.60	n.s.
E	10 000	+80.3	+2.55	+1.6
F	10 000	+145.7	+4.17	+2.5
Blank A	216	+1.9	+0.06	n.s.
Blank B	1000	+4.2	+0.11	n.s.
Blank C	10 000	+9.4	+0.25	n.s.

[a] n.s., not significant.

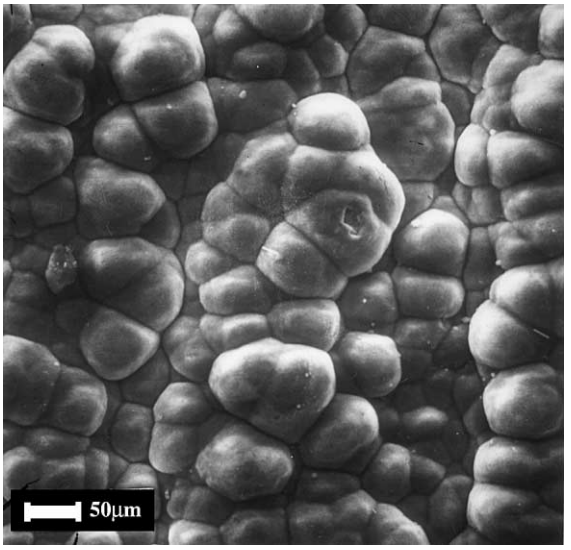

Fig. 3. SiC_f/SiC composite after 1000 h of exposure in Li_4SiO_4 pebble beds, 200×.

Fig. 4. SEM cross-section of SiC_f/SiC composite after 10 000 h of exposure in Li_4SiO_4.

The samples after 1000 h exposure were tested at 400°C and 800°C, and those after 10 000 h only at 800°C. The three-point flexural test results are plotted versus temperature as mean values of 6–10 specimens in Fig. 7(a) (Young's modulus) and Fig. 7(b) (flexural strength). Limited variations were detected. In particular, the flexural strength at 800°C showed a small worsening for samples immersed for 1000 h (just out of the error range) and a worsening of about 25% for samples after 10 000 h of exposure. On the contrary, Young's modulus resulted to be practically unaffected. No significant changes in the elastic properties of blank specimens were observed.

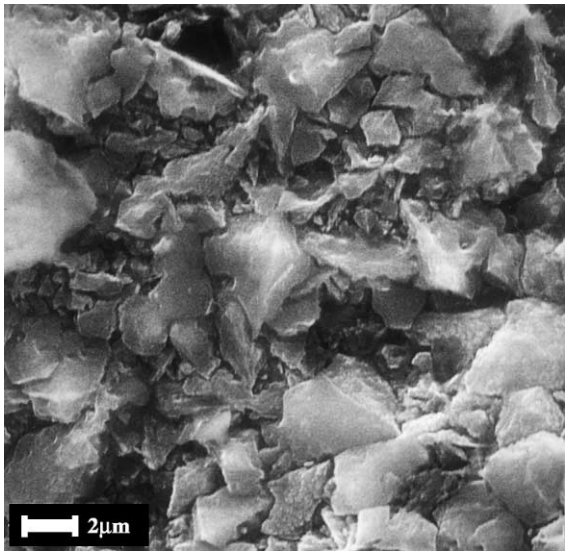

Fig. 5. Blank sample of SiC_f/SiC composite after 216 h over Li_4SiO_4.

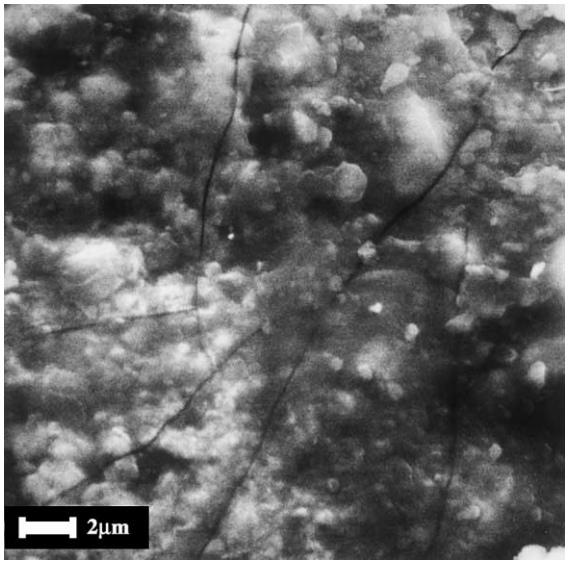

Fig. 6. Blank sample of SiC_f/SiC composite after 1000 h of exposure over Li_4SiO_4, 5000×.

3.1.2. Chemical behaviour

The data relative to the maximum weight change (per unit area) of blank and immersed samples and their squared values estimated on different specimens versus time are shown in Figs. 8(a) and (b). The reaction kinetics study performed by means of weight changes per unit area should be canonically followed on a single specimen, but it was not possible in our case due to the experimental setup. The use of maximum values

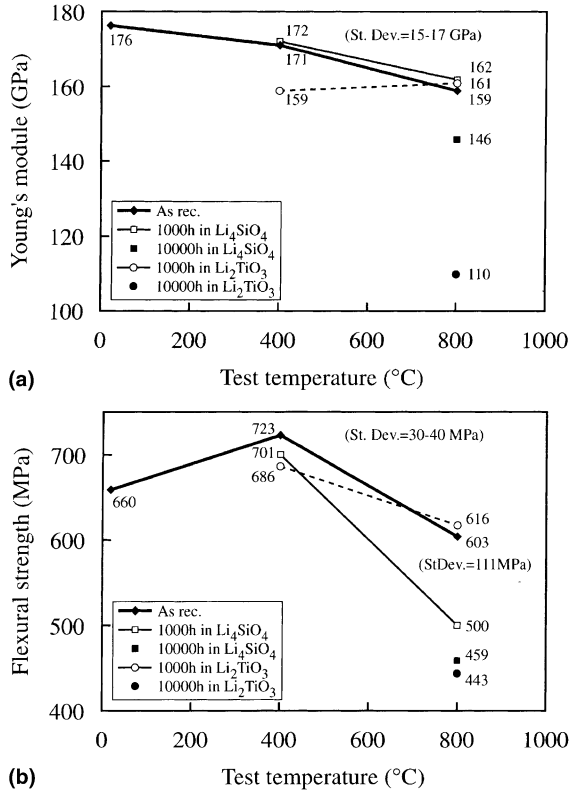

Fig. 7. Mechanical characteristics of SiC_f/SiC composite after exposure in Li_4SiO_4 and Li_2TiO_3: (a) Young's modulus; (b) flexural strength.

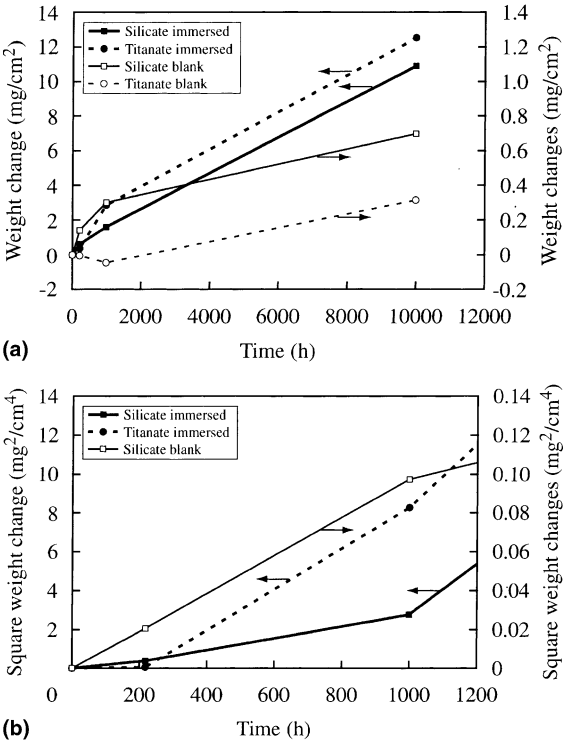

Fig. 8. Weight change (a) and squared weight change (b) of SiC_f/SiC composite after exposure in Li_4SiO_4 and Li_2TiO_3.

(detected on different specimens) can be considered as a conservative approach from an engineering point of view that some considerations can be drawn in any case. Fig. 8(a) shows that the immersed samples after the initial 216 h followed practically a linear weight increase in time, which indicates the existence of a non-protective mechanism controlled by the experimental conditions only (temperature, gas composition, reacting species, etc.) and not by reaction products. Blank samples showed a parabolic weight increase up to 1000 h (Fig. 8(b)), which means that a protective mechanism is operating [11]; subsequently, a different kinetics, with an even lower rate, was observed.

With the aim to state a prediction about the corrosion behaviour of the composite, it is necessary to try to understand the mechanism that is operating. On the grounds of the thermochemical and thermodynamic data stored in the JANAF tables [12], Barin [13] and other recently published data [9,14,15], some conclusions can be drawn, even if further experimental work will have to be performed to understand the global mechanism.

Kleykamp proved that α-SiC does not react with Li_4SiO_4 until up to 1000°C in static argon, whilst in the presence of SiO_2 a solid state reaction starts at 760°C that completely transforms SiC to Li_2SiO_3 when temperature is risen up to 1000°C [15]. In the experimental conditions under study, the outer layer of composite tiles is just SiC and only a very thin layer of SiO_2, that is not detectable by XRD technique, could eventually be present. Then, no reactions between SiC and Li_4SiO_4 should be observed unless silica may be formed in situ during the process. Really, two reactions that are responsible for water production are operating in the system. The first one involves the phase Li_2TeO_3 that is present as a consequence of 2% TeO_2 addition to the pebble [9]. In fact, at low oxygen partial pressure, TeO_2 evaporates from Li_2TeO_3 and decomposes to Te and O_2. Oxygen, then, produces water reacting with hydrogen. Reaction (1) summarises decomposition and water production. A separate test, performed at our laboratory, on the same pebbles at 800°C in He + 0.1% H_2 confirmed these reactions since a mirror of metallic tellurium was observed in the cold zone downstream the pebbles bed. Moreover, water was collected and quantitatively determined [8], whilst no oxygen was detected.

$$TeO_2(g) + 2H_2(g) = Te(g) + 2H_2O(g) \quad (1)$$

$$SiC + 3H_2O(g) = SiO_2 + CO(g) + 3H_2(g) \quad (2)$$

$$SiO_2 + Li_4SiO_4 = 2Li_2SiO_3 \quad (3)$$

$$SiO_2 + Li_2SiO_3 = Li_2Si_2O_5. \quad (4)$$

The second reaction is the reduction of metallic impurities that was quantified and was, for convenience, expressed as Li_4SiO_{4-x}, where $x = 0.04$ [16]. So, depending on the reduction kinetics, water can be internally produced for 1000 h. The produced water vapour together with the amount already present in the purging gas promotes SiC oxidation to SiO_2 following reaction (2). Silica, then, is readily converted into Li_2SiO_3 following reaction (3) when in direct contact with pebbles. The presence of Li_2SiO_3 on blank samples, that were not in contact with the pebble bed, may be explained since, gaseous Li and LiOH have been detected over Li_4SiO_4 in hydrogen atmosphere using Knudsen diffusion mass spectroscopy performed by Yamawaki et al. [17] in a temperature range from 900°C to 1450°C. Then silica, not in contact with Li_4SiO_4, can be joined by such volatile species and transformed to Li_2SiO_3. Finally, the silicate $Li_2Si_2O_5$ is justified by reaction (4).

Summarising, the driving force of the entire corrosion process is the water production. The kinetic mechanism is linear and not protective but its rate is very slow (about 30 μm of SiC coating transformed after 10 000 h) so that the mechanical properties of the composite were practically only slightly affected after 10 000 h.

3.2. Exposure in lithium titanate pebble beds

Immersed samples continuously increased their weight with exposure time (Table 5). The weight increase of specimens after 10 000 h was a bit underestimated since several titanate pebbles remained strongly attached to the sample surfaces, and were detached together with some superficial scale, thus producing large geometrical imperfections. The density did not significantly change until up to 1000 h and was underestimated after 10 000 h due to the above-mentioned imperfections.

SEM observations evidenced a scale that covered a small percentage of the composite surface after 216 h (Fig. 9) and practically the whole surface after 1000 h. In the latter case, the presence of spherical deposits of diameters ranging from few μm up to 200 μm was detected. The specimen texture was almost completely hidden. Fig. 10 shows a very porous surface with white non-conductive spherical deposits and the presence of a cracked thick scale. After 10 000 h the surface appeared completely vitrified and different morphologies were detected on opposite sides of the immersed specimens. On one side, a layer of an almost constant 60–70 μm thickness of the original SiC coating was still present and was covered by a heavily cracked scale about 30 μm thick. On the other side, as can be seen in Fig. 11, the original CVD SiC layer appeared to be completely transformed, it was full of voids with some cracks crossing its entire thickness. The SiC fibres after 10 000 h are no longer protected and thus exposed to the reacting environment.

A very little amount of Li_2SiO_3 phase was evidenced by XRD analysis on samples after 216 h. Silica and $Li_2Si_2O_5$ were also detected in increasing amounts on specimens exposed for longer periods. Only Li_2SiO_3 and TiO_2 phases but no TiC phase were observed on pebbles even after 10 000 h. Blank samples were practically unchanged until up to 1000 h, and after 10 000 h exposure only very slight or no variations of weight, density and elastic properties were observed. A smoothing of the original surface of the CVD SiC crystal morphology was observed after 1000 h but no other phases than SiC were detected. After 10 000 h a thick cracked scale of silica was identified by XRD.

3.2.1. Mechanical properties

No changes in the elastic properties were detected after 216 h of exposure. On the contrary, their worsening in time was observed. The dynamic Young modulus was 3% and 8.5% lower after 1000 and 10 000 h, respectively, while the dynamic torsional modulus is worsened by 4–7% and 17%. Even the damping constant changed by about 500–600% after 1000 h and by more than 700%

Table 5
Weight and density variation of blank and immersed specimens in Li_2 TiO_3

Specimen	Exposure time (h)	Weight variation (mg)	Weight variation (%)	Density variation (%)
A	216	+2.5	+0.07	n.s.[a]
B	216	+2.2	+0.06	n.s.
C	1000	+20.7	+0.55	n.s.
D	1000	+39.8	+1.07	n.s.
E	10 000	+130.7	+3.50	−5.6
F	10 000	+167.7	+4.74	−3.7
Blank A	216	−0.1	<−0.01	n.s.
Blank B	1000	−0.6	−0.02	n.s.
Blank C	10 000	+4.2	+0.11	n.s.

[a] n.s., not significant.

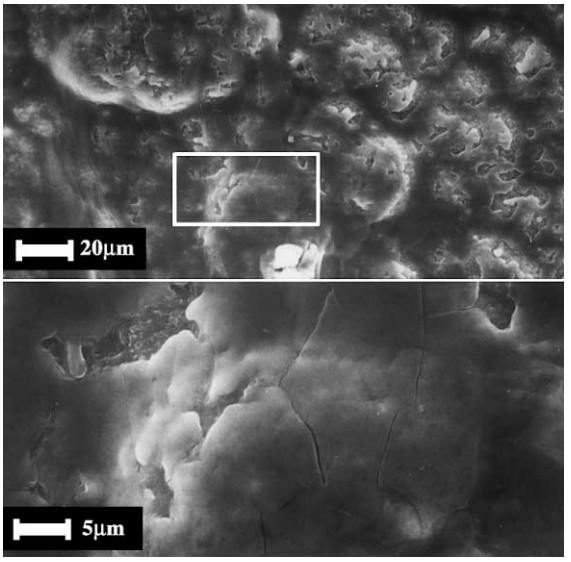

Fig. 9. SiC_f/SiC composite after 216 h of exposure in Li_2TiO_3, 500/2000×.

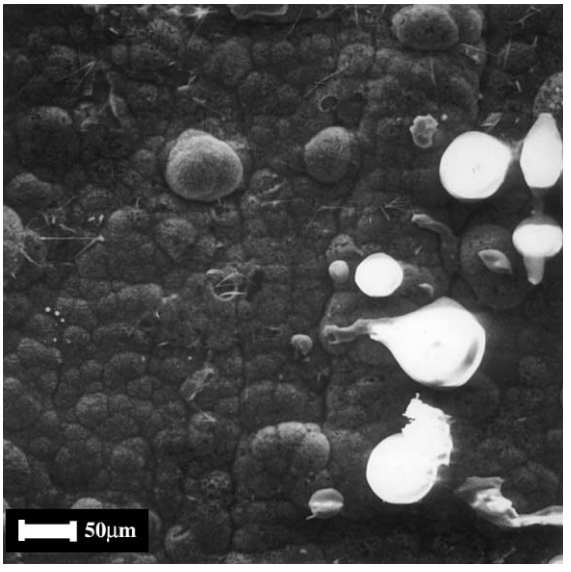

Fig. 10. SiC_f/SiC composite after 1000 h of exposure in Li_2TiO_3, 200×.

after 10 000 h, thus indicating a defect population increase.

Finally, Fig. 7 shows a summary of the mechanical data obtained by the three-point flexural test. In the upper side, the static Young's modulus after 10 000 h of exposure appeared to decrease by 30.8% at 800°C, whilst no significant changes were present after 1000 h. Similarly, the flexural strength was unchanged after 1000 h and was reduced by 26% after 10 000 h with respect to samples in the as-received conditions.

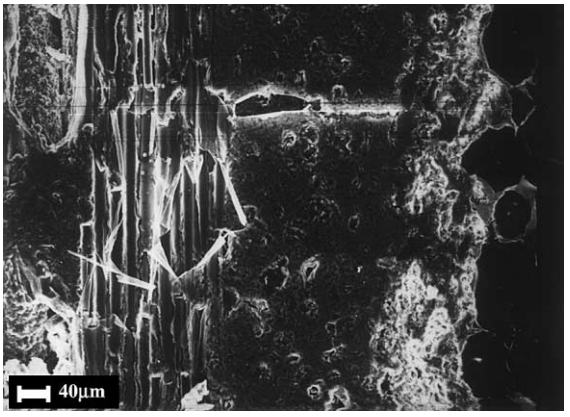

Fig. 11. SEM cross-section of SiC_f/SiC composite after 10 000 h of exposure in Li_2TiO_3.

3.2.2. Chemical behaviour

Data relative to the weight change per unit area of blank and immersed samples, and their squared values against time, are shown in Fig. 8 for samples exposed in contact with lithium titanate. Both blank and immersed samples show two different reaction kinetics.

In the case of immersed samples, a change of the corrosion rate was observed between 216 and 1000 h showing a kinetic law higher than quadratic. Initially the rate was lower than that was observed in the silicate pebbles bed, then, the two rates became similar. In any case, no protective mechanism was operating, as confirmed by the consumption of the CVD SiC protective layer previously observed (Fig. 11).

Concerning the blank samples no clear kinetic laws were noted. A weight decrease until up to 1000 h and a successive weight increase was observed probably following a linear kinetic law. The initial weight decrease and the XRD analysis could be explained only if active oxidation of SiC was operating, but to confirm this hypothesis, it is necessary to perform further work. After 1000 h, a sufficiently oxidising gas phase went in contact with the blank sample to produce silica phase on its surface, as it is suggested by the positive weight change observed. No lithium compounds were detected on the blank sample, so indicating a lower volatility with respect to the system containing Li_4SiO_4.

The mechanism of SiC oxidation for immersed samples could include the reaction $SiC + Li_2TiO_3 = TiC + Li_2SiO_3$ that is energetically favoured ($\Delta G = -84.5$ kJ mol^{-1} at 800°C), but no TiC was detected in all the composite specimens and pebbles after their use in the test. So, even in the system with Li_2TiO_3, water formation must be the first step of the entire mechanism

$$Li_2TiO_3 + xH_2(g) = Li_2TiO_{3-x} + xH_2O(g) \quad (5)$$

$$SiO_2 + Li_2TiO_3 = Li_2SiO_3 + TiO_2. \quad (6)$$

Li_2TiO_3 reduction, as reported in reaction (5), is the only possible way to produce water. Then, silica formed following reaction (2) can be transformed by Li_2TiO_3 into Li_2SiO_3 following reaction (6), as it was observed in our laboratory experiments, where quartz containers reacted with Li_2TiO_3 at 800°C in He + 0.1% H_2 flow. Anyway, considering the pebble amount in a cell, their reduction kinetics and the gas flux, water production should be exhausted in less than 216 h, though this was not observed in the experiment. The amount of Li_2TiO_3, as an oxygen supplier, is not sufficient to justify the SiC oxidation after 216 h; it must therefore be concluded that after the operations to disconnect the first cell, air contamination took place in the loop with cells containing Li_2TiO_3. An indirect confirmation was obtained through the chemical reduction degree of the pebbles after exposure. The chemical reduction degree after 216 h was about twice the ones after 1000 and 10 000 h.

4. Conclusions

SiC-coated SiC_f/SiC composite samples were exposed to Li_4SiO_4 and Li_2TiO_3 pebble beds in fusion relevant conditions for 216, 1000 and 10 000 h.

Elastic and mechanical characteristics were measured both on as-received samples and after exposure, in order to determine, if any, their variations.

For samples exposed to Li_4SiO_4 after 10 000 h, no changes in the dynamic Young's modulus and a light worsening of the dynamic torsional modulus were observed, whilst the flexural strength showed a worsening of about 25%. In the experimental conditions the transformation of the SiC coating was not a protective one. However, a significant fraction of the original SiC coating was still present after 10 000 h. Only about 30 μm layer was transformed into Li_2SiO_3, and the fibres were not yet exposed to the environment. Thus, a long lifetime can be foreseen for such a kind of composite depending on the SiC coating thickness.

Concerning samples exposed to Li_2TiO_3, a very low weight increase was observed on samples up to 1000 h and practically no variations of elastic and mechanical properties were observed. On the contrary, after 10 000 h a sharp change of weight increase was surprisingly noticed with the SiC coating that appeared totally transformed and the SiC fibres were exposed to the environment. Elastic and mechanical properties appeared degraded. Samples relative to 10 000 h exposure were likely affected by an accidental air contamination; therefore, the disappointing long term behaviour of the material could have been markedly affected and possibly entirely due to that air contamination.

References

[1] S. Sharafat, F. Najmabadi, C.P.C. Wong, ARIES Team, Fus. Eng. Design 18 (1991) 215.
[2] S. Ueda, S. Nishio, Y. Seki, R. Kurihara, J. Adachi, S. Yamazaki, DREAM Design Team, J. Nucl. Mater. 258–263 (1998) 1589.
[3] A.S. Peres Ramirez, A. Caso, L. Giancarli, N. Le Bars, G. Chaumat, J.F. Salavy, J. Szczepanski, J. Nucl. Mater. 233–237 (1996) 1257.
[4] T. Sample, P. Fenici, H. Kolbe, L. Orecchia, J. Nucl. Mater. 212–215 (1994) 1529.
[5] A. Caso, P. Huet, P.C. Tramier, in: Proceedings of the IEA International Workshop on SiC/SiC Ceramic Composite for Fusion Structural Applications, 28/29 October 2000, Ispra (VA), Italy.
[6] G. Zener, Elasticity and Anelasticity of Metals, University Chicago, 1948.
[7] M. Dalle Donne, European DEMO BOT Solid Breeder Blanket, KfK 5429, 1994.
[8] C. Alvani, P.L. Carconi, S. Casadio, A. Moauro, C.A. Nannetti, F. Pierdominici, Interaction chemistry of purge gas with Li_4SiO_4 pebbles. Sub-TASK WP B8-3.3 1997 Activity Report, Doc. ENEA INN/NUMA/MATAV 1, 1998.
[9] H. Kleykamp, Z. Metalld. 90 (1999) 837.
[10] N. Roux, et al., Low temperature tritium releasing ceramics as potential materials for the ITER breeding blanket, in: Proceedings of the International Workshop on Ceramic Breeder Blanket Interaction, Kyoto Japan, October 9–11, 1995.
[11] P. Kofstad, High Temperature Corrosion, Elsevier, Amsterdam, 1988, p. 18.
[12] M.W. Chase, et al., JANAF Thermochemical Tables, third Ed., J. Phys. Chem. Reference Data vol. 14, suppl. 1, 1985.
[13] I. Barin, Thermochemical Data of Pure Substances, 2nd Ed., VCH, Weinheim, 1993.
[14] S. Claus, H. Kleykamp, W. Smykatz-Kloss, J. Nucl. Mater. 230 (1996) 8.
[15] H. Kleykamp, J. Nucl. Mater. 283–287 (2000) 1385.
[16] C. Alvani, P.L. Carconi, S. Casadio, A. Moauro, J. Nucl. Mater. 280 (2000) 372.
[17] M. Yamawaki, A. Suzuki, M. Yasumoto, K. Yamaguchi, J. Nucl. Mater. 247 (1997) 11.